Journal of the European Ceramic Society 22 (2002) 1775–1782

www.elsevier.com/locate/jeurceramsoc

Processing of cordierite based ceramics from alkaline-earth-aluminosilicate glass, kaolin, alumina and magnesite

D.U. Tulyaganov[a], M.E. Tukhtaev[a], J.I. Escalante[b], M.J. Ribeiro[c], J.A. Labrincha[d,*]

[a]*Chemical Technological Institute, 700000, Tashkent, Uzbekistan*
[b]*Centre for Research and Advanced Studies, Saltillo, Mexico*
[c]*ESTG, Polytechnic Institute of Viana do Castelo, 4900 Viana do Castelo, Portugal*
[d]*Ceramics and Glass Engineering Department, UIMC, University of Aveiro, 3810-193 Aveiro, Portugal*

Received 27 June 2001; received in revised form 26 October 2001; accepted 11 November 2001

Abstract

Microstructural changes, porosity evolution and properties of cordierite based composites have been studied as a function of cordierite–anorthite ratio in modelled ceramic systems. The model systems were composed of alkaline-earth-aluminosilicate glass powder, kaolin, alumina and magnesite. Suitable densification levels of investigated compositions are attained in a narrow temperature range and relatively high residual porosity levels are observed. These features were attributed to the role of the liquid phase during high temperature sintering. Cordierite, anorthite or mixtures of each with mullite are the formed crystalline phases when maximum densification levels are achieved. Their properties are correlated to the processing route and to the composition of sintered materials. Control of the porous structure through manipulation of heating rate was found feasible and easy to implement.

Keywords: Anorthite; Cordierite; Glass ceramics; Microstructure-final; Mullite; Porosity; Sintering

1. Introduction

Cordierite-based ceramics have been prepared by sintering or by using the glass-ceramic approach, starting from a large variety of materials.[1–3] Despite numerous attempts and extensive research, cordierite bodies are still under study[4–7] because of their high volume resistivity ($>10^{14}$ Ω cm), and low linear thermal expansion ($\leqslant 2\times10^{-6}$/K, between 20 and 800 °C) and tentative attempts to control and improve preparation processes (e.g., by using cheaper precursors). Cordierite composition varies between the limits expressed by the formulas $2MgO{\cdot}2Al_2O_3{\cdot}5SiO_2$ and $MgO{\cdot}Al_2O_3{\cdot}3SiO_2$. However, samples in this range tend to show abrupt maturation processes and their production is difficult to control.[8] Moreover, relevant properties of cordierite ceramics seem to be strongly dependent on the composition, nature of raw starting materials and the presence of impurities and additives, and also the fabrication technique. Secondary crystalline phases like mullite, corundum, spinel, forsterite, clinoenstatite, crystobalite are often present, together with a glassy phase and this complex final mixture determines the properties of the samples.

The main purpose of the present study is to produce cordierite based ceramics with anorthite as the main secondary phase, changing the cordierite–anorthite ratio in modelled systems. These systems are composed of different mixtures of an alkaline-earth-aluminosilicate glass powder, kaolin, alumina and magnesite. Preliminary work has been developed[9] and has demonstrated the adaptability of this approach. However, the ability to control and adjust the microstructure and relevant properties of the final material is still required.

2. Experimental procedure

Alkaline-earth-aluminosilicate glass powder having an average chemical composition (wt.%) of 46.81 SiO_2, 15.35 Al_2O_3, 0.62 Fe_2O_3, 0.28 TiO_2, 24.51 CaO, 9.64 MgO, 0.41 Na_2O, 0.04 K_2O, 2.00 P_2O_5, and 0.34 CaF_2 was used as the fluxing agent. This glass composition corresponds to the $CaAl_2Si_2O_8$–$CaMgSi_2O_6$ boundary of the fluorapatite–anorthite–diopside system[10] and was

* Corresponding author. Tel.: +351-234370250; fax: +351-234425300.
E-mail address: jal@cv.ua.pt (J.A. Labrincha).

0955-2219/01/$ - see front matter
PII: S0955-2219(01)00506-4

previously applied in the production of wear-resistant glass-ceramic materials.[11] A wet-cycloned classified kaolin (the raw kaolin is obtained by open cast coal mining in Angren deposit, Uzbekistan) with a kaolinite content of 65 wt.%, 25 wt.% of quartz, and mica, feldspar, carbonates, and iron-containing minerals as minor components was also used. Its average chemical composition (wt.%) is: 58.77 SiO_2, 25.85 Al_2O_3, 1.75 Fe_2O_3, 0.58 TiO_2, 0.50 CaO, 0.22 MgO, 0.10 Na_2O, 1.00 K_2O, 0.07 P_2O_5, and 10.90 L.O.I. Industrial grade alumina (wt.% chemical composition: 96.17 Al_2O_3, 0.10 TiO_2, 0.84 CaO, 0.14 MgO, 0.19 SO_3, 0.49 Na_2O, 0.10 K_2O, and 2.12 L.O.I.) and magnesite (~99 wt.% pure) were the complementary reagents.

The model systems were obtained from batch formulations containing variable proportions of the mentioned precursors (Table 1) and fixed cordierite-anorthite ratios (wt.%): 50:50, 70:30 and 90:10, named C-1, C-2, and C-3, respectively.

Magnesite was crushed and then wet milled with alumina and glass-powder in a porcelain ball mill, loaded with pebbles, raw materials and water (wt.% ratio of 1:1:1). Kaolin and ball clay were previously washed, and then added to the non-plastic components. The milling process was assumed correct when the residue by sieving at 63 μm was lower then 1%. De-watering process of milled suspension took place in a plaster mould. Final water contents of about 21–23 wt.% were achieved. Moderately plasticity levels of all batches permit the use of traditional plastic forming shaping methods. When necessary, small amounts of a common ball clay were added. After shaping, samples were left to dry at room temperature for about 24 h and then were placed at 110 °C in a laboratory drier for another 24 h. Composition (both chemical and mineralogical) and properties evolution was studied with samples fired at 900, 1100, 1200 and 1300 °C in an electrical lab-scale furnace and on changing the heating rate (2–10 °C/min). Maximum sintering temperature changed from 1350 to 1410 °C depending on the composition. A chamber gas kiln that permits the use of oxidizing or reducing atmospheres (adjusted by changing air/gas proportion in the burners) at different stages of the firing process (complete cycle duration of 24 h and soaking time of 1 h) was also used.

Crystalline phases formed were identified by XRD in the 5–40 ° 2θ range using a Cu-tube difractometer (Philips X'PERT, PW3040). Microstructural evaluation of sintered samples was conducted by scanning electron microscopy (SEM—Jeol 5800 LV) and by reflected light microscopy. Polished samples were etched by dipping for 1 min in a 5 vol.% HF solution, then washed in water and finally carbon or gold coated. The chemical composition, including distribution and relative proportions of phases, was determined by an X-ray microanalyser (EDS- S60 DX90) coupled to the SEM. The porosity was evaluated from the microstructure using a common stereological point counting method.[12] Flexural strength was determined using a three-point bending test on rectangular cross section bars (3×3×40 mm). Dilatometric studies were conducted in a Netzsch 402EP dilatometer at a constant heating rate of 10 °C/min. The electrical specific resistance was measured by 2-probe impedance spectroscopy (HP4284A potentiostat). The bulk density was measured by the Hg-immersion Archimedes method. Finally, drying and firing linear shrinkages, and water absorption of samples were determined by common means.

Table 1
Tested batch formulations (wt.%)

Components	C-1	C-2	C-3
Glass powder	37.23	21.35	6.72
Kaolin	42.08	49.70	63.20
Alumina	15.29	13.38	10.80
Magnesite	5.40	12.67	19.34
Ball clay	–	3.00	–

3. Results and discussion

3.1. Sintering behaviour of C-1 composition

The sintering of C-1 samples was carried out at temperatures 900, 1100, 1200, 1300 and 1350 °C for 1 h with heating rate 1.5–2.0 °C/min. No evidence of densification was observed after firing at 900 °C. Samples show linear shrinkage values of only about 0.8%, very high water absorption levels (53.3%), and small bending strength values (7.21 MPa). Crystalline phases detected in these samples include α-quartz and corundum (Fig. 1 A). Between 1100 and 1200 °C, the process of incipient densification starts to occur due to the liquid phase flowing. At 1100 °C strong anorthite, and weak diopside and enstatite peaks are detected in the X-ray diffraction patterns (Fig. 1B). Decreasing intensity of the α-quartz peaks and disappearance of diopside peaks at 1200 °C are related with dissolution reactions in the liquid phase. Cordierite is formed at 1300 °C and its amount tends to increase at higher temperatures (1350 °C). The X-ray diffraction pattern of the final product consists of hexagonal α-cordierite (e.g. indialite), triclinic anorthite, and α-alumina peaks (Fig. 1D).

Maximum densification levels are obtained in a narrow temperature range (1320–1350 °C) because of the abrupt formation of liquid phase. After firing, samples are distinguished by their vitreous nature due to a strong self-glazing effect. Even using slow heating rates (1.5-2 °C/min) as an attempt to reach highest density levels, sintered products exhibit densification levels of 88% and about 14 vol.% of residual porosity after heat treatment at 1350 °C. The possible cause for this high

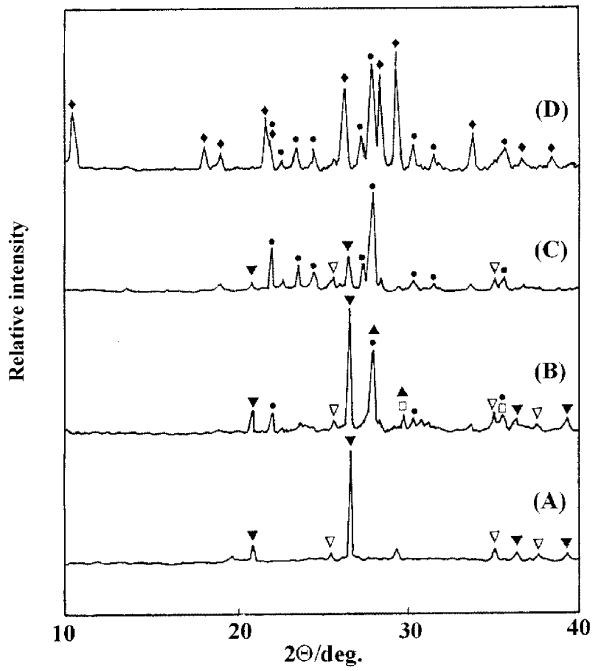

Fig. 1. XRD spectra of C-1 samples fired at different temperatures: (A) 900 °C; (B) 1100 °C; (C) 1200 °C; (D) 1350 °C. Detected phases: (◆) cordierite; (•) anorthite; (□) diopside; (▼) α-quartz; (▲) enstatite; (▽) α-alumina.

porosity can be the vapour derived from volatilisation or decomposition reactions of some starting materials, such as kaolinite and magnesite. Obviously, released gases might be partly trapped by the softened alkaline-earth-aluminosilicate glass (dilatometric softening temperature of about 750 °C).

A representative SEM view of sintered bodies is shown in Fig. 2 A, confirming the presence of considerable amount of pores (bubbles). EDS analysis of mottled crystals grains gives the average composition (wt.%): 52.05 SiO_2, 33.44 Al_2O_3, 1.87 FeO, 1.54 CaO, 10.36 MgO, and 0.74 K_2O. This composition is close to cordierite crystalline phase (pure cordierite consists of 51.36% SiO_2, 34.86% Al_2O_3, and 13.78% MgO). In this approach, Fe^{3+} to Fe^{2+} reduction was assumed due to the reducing character of the kiln atmosphere, and subsequently FeO for MgO substitution occurs in the cordierite structure. Relatively high contents of CaO and K_2O were related to the embedding of cordierite crystals in the glassy phase. Clusters of another crystalline phase were also observed under higher magnification (some of those are identified as "a" in Fig. 2B). The chemical composition (wt.%) is now 45.64 SiO_2, 33.40 Al_2O_3, 0.74 FeO, 18.78 CaO, 0.26 Na_2O, and 0.48 K_2O, and corresponds to anorthite (pure anorthite consists of 43.19% SiO_2, 36.65% Al_2O_3 and 20.16% CaO). The microcracks observed inside and along cordierite grains can be a consequence of the polishing or etching treatments but their primary probable cause is the partial dissolution in the glassy phase. Typical microstructural details of cordierite-

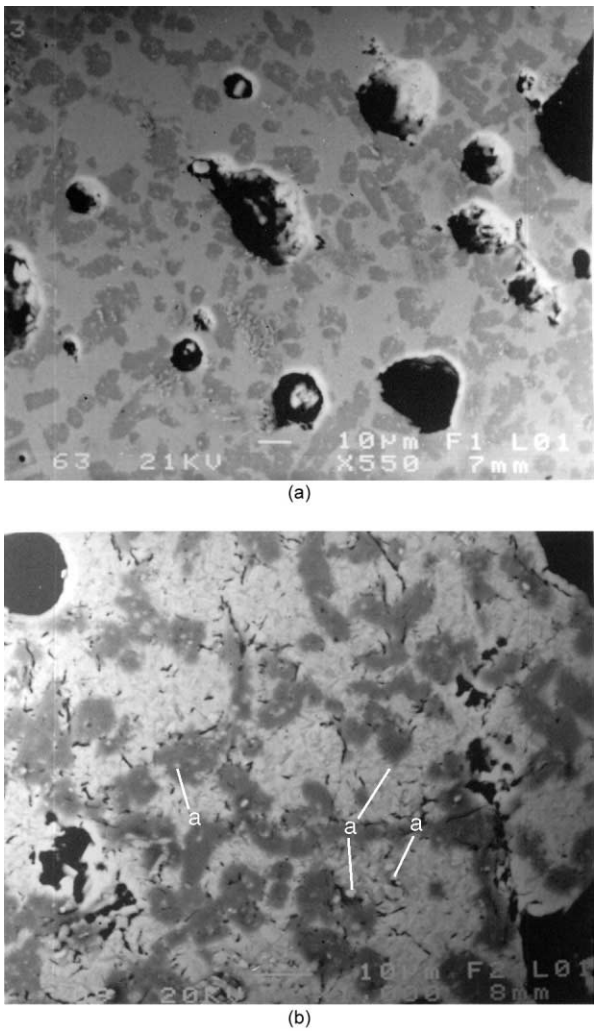

Fig. 2. SEM images of C-1 sample fired at 1350 °C, obtained at different magnifications: (a) 550×; (b) 1000× (a—anorthite).

based ceramics such as the presence of microcracks are attributed to intercrystalline stresses resulting from the thermal expansion anisotropy of crystalline cordierite.[2] Another possible explanation is the thermal expansion mismatch between cordierite and anorthite, whose thermal expansion coefficient is about 4.3×10^{-6}/K between 20 and 500 °C. However, other mullite-cordierite composites having higher thermal mismatch only show minor species dislocations and absence of cracks.[13]

Relatively high residual porosity values of sintered products (even at 1350 °C) deserve a further control of microstructural evolution. A simple change in the sintering schedule (faster heating rates of 5 and 10 °C/min and electrically heating means) seemed to be suitable. A strong increase of porosity levels was obtained after heat treatment at 1300 °C (Fig. 3A and B), but the pores are mostly closed and complete densified ceramic bodies were produced. Moreover, the pore structure is strongly homogeneous but the size range is vast (0.01–1000 μm). Apparent density of sintered products changes from 34

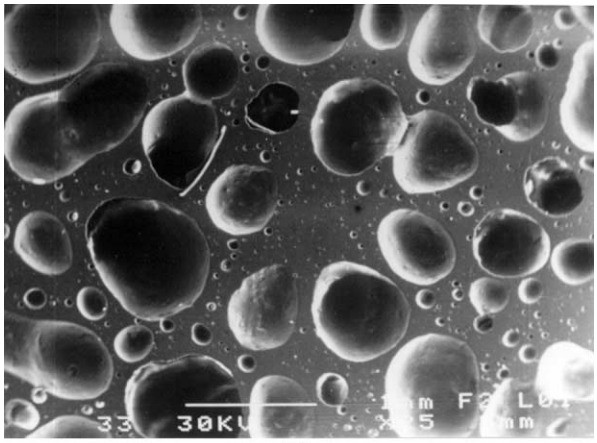

Fig. 3. Optical microscopy images of C-1 samples fired at 1300 °C under different heating rates: (A) 5 °C/min; (B) 10 °C/min.

to 38% of the theoretical value. The further increase of temperature causes deformation and loss of shape.

A representative SEM view of the crystalline matrix between pore walls is shown in Fig. 4 A, where needle-like and leaf-like crystals embedded in a crystalline matrix are noticed. A highly magnified view of the crystalline matrix (Fig. 4B) shows the formation of anorthite plate-like crystals, such as those observed in bone-china porcelain[14] and in cordierite–glass ceramic substrates used for ruthenia-based resistors.[7] EDS analyses of anorthite crystals give the following average composition (wt.%): 53.38 SiO_2, 25.49 Al_2O_3, 0.75 TiO_2, 1.72 Fe_2O_3, 13.10 CaO, 3.89 MgO, 1.35 K_2O, and 0.33 Na_2O. These values are somewhat different from the stoichiometric anorthite composition, probably due to the proximity of a silica-rich glassy phase, with average chemical composition (wt.%) 48.69 SiO_2, 30.22 Al_2O_3, 1.00 TiO_2, 2.17 Fe_2O_3, 11.93 CaO, 4.39 MgO, and 1.60 K_2O. Needle-like and leaf-like crystals were respectively assumed as mullite and aluminate spinel phases (Fig. 4C and D).

Fig. 5 shows XRD spectra of C-1 samples sintered under different heating conditions. Spectra of porous products (Fig. 5B) show anorthite as the major phase formed after firing at 1300 °C. Additionally, very small alumina and spinel peaks were observed. Cordierite formation was not detected even after increasing the soaking time up to 1.5 h. The modification of the sintering schedule strongly changes both the porosity and the phase relationship of the material, for reasons still not very well defined. Liquid phase formation might be responsible and becomes important in the temperature range of 1200–1250 °C, where the alkaline earth-aluminosilicate glass is less viscous than 10^2 Pas.[11] Obviously, gas trapping by the melt is intensified in the early stages of densification when faster heating rates are used. This glass shows a linear thermal expansion value (calculated as 4.35×10^{-6}/K, between 20 and 400 °C) close to the anorthite phase.

3.2. Sintering behaviour of C-2 and C-3 compositions

The sintering schedule for C-2 and C-3 samples was selected to promote maximum densification. Thus, only relatively slow heating rates (1.5–2 °C/min) were used. Fig. 6A and B shows the evolution of relevant parameters as a function of the sintering temperature. Decreasing the amount of liquid phase formed from the alkaline-earth-aluminosilicate glass, especially on composite C-3, inhibits the essential wetting process of solid particles. The driving force for densification that derives from capillary pressure of the liquid phase is subsequently weaker and might not act.[15] Reasonable sintering levels were achieved at 1350 °C when the primary liquid phase appears in the $MgO–Al_2O_3–SiO_2$ ternary system.[16] On heating at 1355 °C, which corresponds to the ternary eutectic temperature, approximately 25 wt.% melt would be expected to form. Complete densification of C-2 samples is achieved at 1380 °C, while C-3 composition requires higher temperatures (1410 °C). In both cases, the densification process strongly develops in a narrow temperature range, as has also been observed for C-1 composition. Final densification levels of 88.5 and 87% are achieved for C-2 and C-3 compositions, respectively. A considerable amount of residual pores, mostly closed, are again retained. The direct relationship between densification and flexural strength evolution is noticed in Fig. 6B.

XRD analysis was carried out only for reasonably densified samples. Results of C-2 samples fired at 1350 and 1380 °C (Fig. 7) show almost invariant peaks intensity of mullite, and anorthite phases with increasing sintering temperature. However, peak intensity of α-cordierite tends to slightly decrease. Thus, the crystallization process seems to proceed faster than the densification mechanism. On C-3 samples, α-cordierite and mullite become the major phases after firing at 1350 °C (Fig. 8). Only very small anorthite peaks are observed at 1380 °C as a consequence of insignificant occurrence of structural

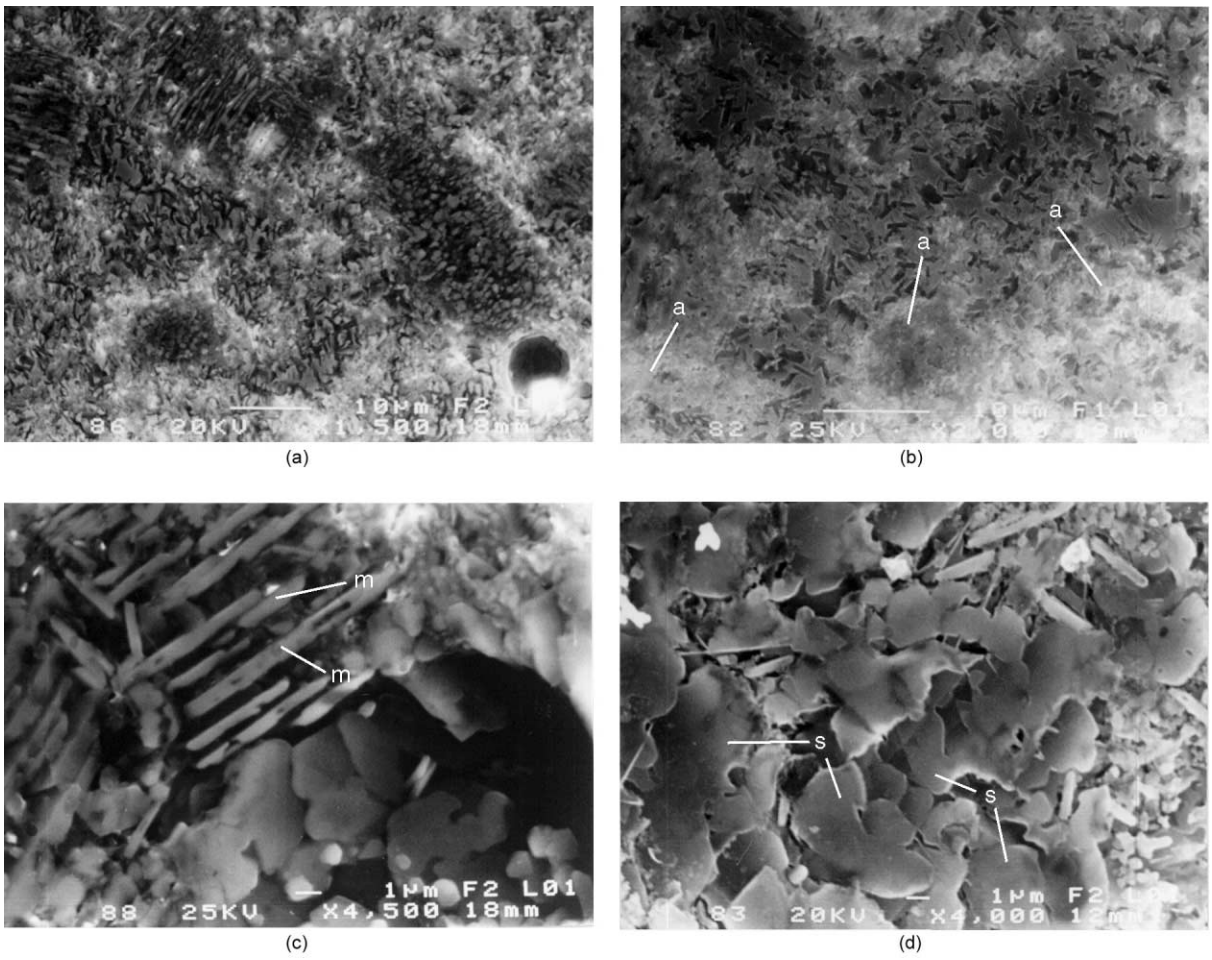

Fig. 4. Typical microstructures (SEM) of C-1 samples sintered at 1350 °C: (A) general view of crystalline matrix between pore walls; (B) plate-like anorthite crystals—a; (C) mullite crystals—m; (D) spinel crystals—s.

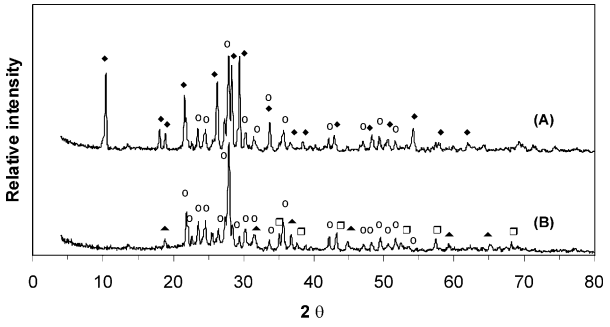

Fig. 5. XRD spectra of C-1 samples fired at 1300 °C under different heating rates: (A) 1.5–2 °C/min; (B) 5 °C/min. Detected phases: (υ) cordierite; (○) anorthite; (□) α-alumina; (▲) spinel.

rearrangements between crystalline phases after reactive-liquid sintering. Crystallinity of those phases enhances with further increases of firing temperature up to 1410 °C.Typical microstructure of C-3 sintered material consists of mottled cordierite grains surrounded by the glass matrix (Fig. 9).

Generally it might be assumed that the thermal expansion of a composite material is roughly equal to the sum of each individual phase multiplied by its respective volume fraction.[2] The decreasing slope of dilatometric curves of C-3 samples sintered at higher temperatures seems to confirm the formation of increasing amounts of cordierite (Fig. 10). As predicted, C-3 samples present the lowest values amongst all the investigated compositions (Fig. 11). The values are relatively stable on the measured temperature range, varying from 2.63×10^{-6}/K between 20 and 700 °C to 2.64×10^{-6}/K between 20 and 1000 °C.

Relevant properties of C-1, C-2, and C-3 samples sintered at respectively adequate temperatures of 1350, 1380 and 1410 °C, are given in Table 2.

3.3. Reaction mechanism and properties evolution

Taking into account that SiO_2, Al_2O_3, CaO and MgO oxides are the main components of the glassy-powder used in this study (96% of chemical composition), calculated molecular formula of the formed glassy phase is 1.6 $MgO{\cdot}3CaO{\cdot}Al_2O_3{\cdot}5.25SiO_2$. Summary reactions between precursors after kaolinite dehydroxylation and magnesite decomposition processes can be described as follows.

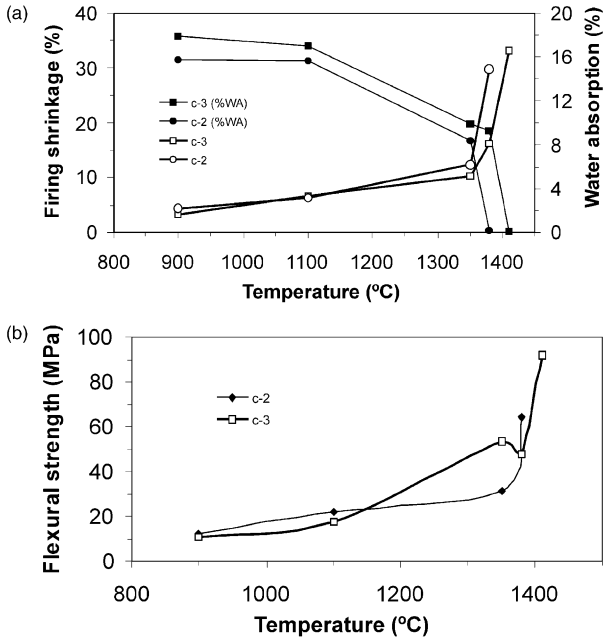

Fig. 6. Properties evolution of C-2 and C-3 compositions as a function of firing temperature: (a) shrinkage and water absorption; (b) flexural strength.

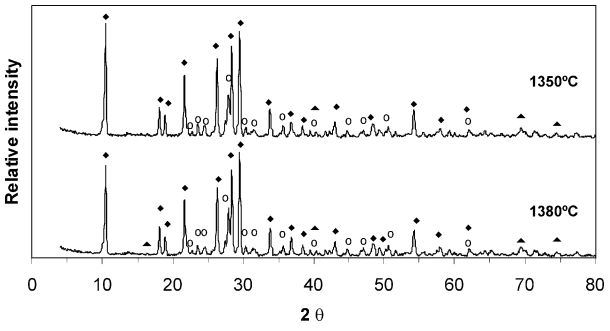

Fig. 7. XRD paterns of C-2 composition fired at different temperatures. Detected phases: (◆) cordierite; (□) anorthite; (▲) mullite.

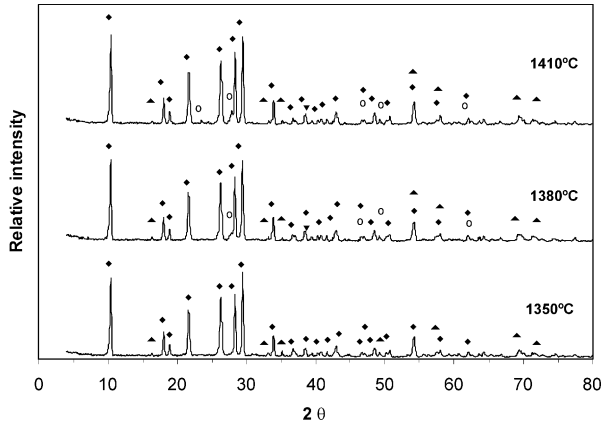

Fig. 8. XRD paterns of C-3 composition fired at different temperatures. Detected phases: (◆) cordierite; (□) anorthite; (▲) mullite.

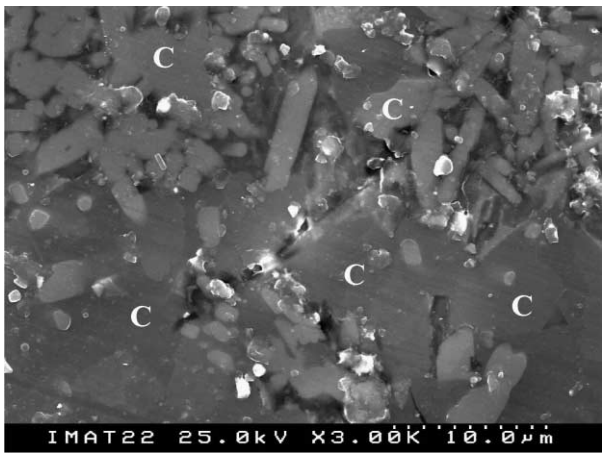

Fig. 9. Representative microstructural (SEM) view of C-3 sample fired at 1410 °C (C—cordierite).

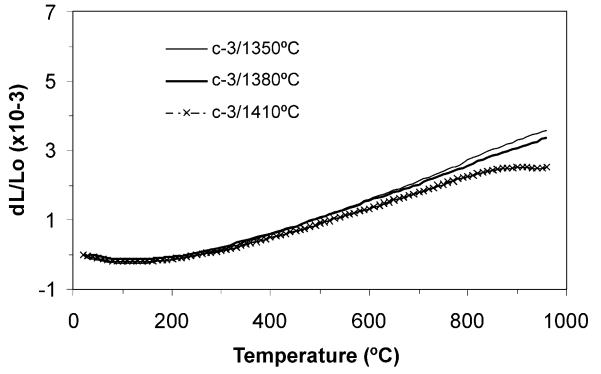

Fig. 10. Dilatometric curves of C-3 samples fired at different temperatures.

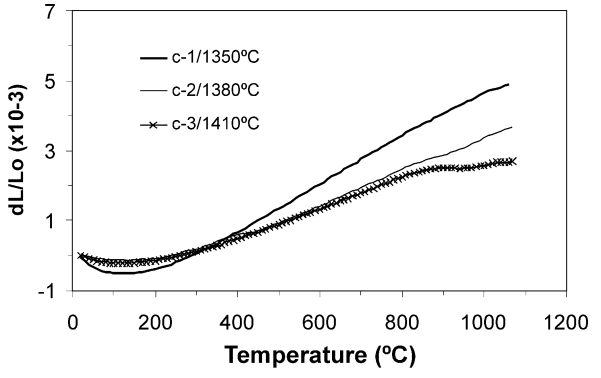

Fig. 11. Dilatometric curves of C-1, C-2 and C-3 samples fired, respectively, at 1350, 1380, and 1410 °C.

(i) Model system C-1:

$$\begin{aligned} &3.5(1.6MgO\cdot 3CaO\cdot Al_2O_3\cdot 5.25SiO_2)\\ &+8(Al_2O_3\cdot 2SiO_2)+4.4MgO+9Al_2O_3\\ &+11.625SiO_2 \;\rightarrow\; 5(2MgO_2\,Al_2O_3\cdot 5SiO_2)\\ &+10.5(CaO\cdot Al_2O_3\cdot 2SiO_2) \end{aligned} \quad (1)$$

(ii) Model system C-2:

$$3.3(1.6MgO\cdot 3CaO\cdot Al_2O_3\cdot 5.25SiO_2) + 16.5(Al_2O_3\cdot 2SiO_2) + 16.72MgO + 12.1Al_2O_3 + 24.475SiO_2 \rightarrow 11(2MgO\cdot 2Al_2O_3\cdot 5SiO_2) + 9.9(CaO\cdot Al_2O_3\cdot 2SiO_2) \quad (2)$$

(iii) Model system C-3:

$$1.6MgO\cdot 3CaO\cdot Al_2O_3\cdot 5.25SiO_2 + 18(Al_2O_3\cdot 2SiO_2) + 24.1MgO + 9.7Al_2O_3 + 29SiO_2 \rightarrow 12.85(2MgO\cdot 2Al_2O_3\cdot 5SiO_2) + 3(CaO\cdot Al_2O_3\cdot 2SiO_2) \quad (3)$$

These reactions correspond to stoichiometric relations between precursors and sintered products but, in practice, could not accurately represent the real reaction mechanism occurring upon firing. However, they might be used to explain the observed relative phase evolution between tested compositions.

Model system C-1 was chosen to illustrate the simplified sequence of reactions that occur upon sintering:

(i) *Up to 900 °C*: dehydroxylated clay, magnesia, quartz, alumina and softened glass particles are present.

(ii) *At about 1100 °C*: devitrification of the alkaline-earth glass, and anorthite + diopside crystallization occur. Clay relicts, quartz, alumina and magnesia particles remain practically stable, and incipient precipitation of enstatite crystals might be observed as a consequence of reaction of quartz towards magnesia.

(iii) *Between 1200 and 1300 °C*: the viscosity of the remaining liquid phase abruptly decreases and dissolution of clay relicts, diopside, enstatite and major quantity of quartz crystals is strongly improved. Anorthite becomes the major crystalline phase and MgO, SiO_2, and Al_2O_3 enrichment of liquid phase is predictable. At 1300 °C cordierite crystals started to precipitate from this complex melt.

(iv) *Above 1300 °C*: cordierite and anorthite crystals + liquid phase are present.

For the same composition, the use of a relatively higher heating rate in the interval 1200–1300 °C strongly changes the reaction mechanism in the sense that no cordierite formation is observed. Above 1300 °C anorthite becomes the major phase in these highly porous materials.

Reaction sequence for C-2 composition is considerably similar to that described for C-1 material. However, when anorthite crystals precipitate via devitrification of the alkaline-earth-aluminosilicate glass, the amount of remaining liquid phase might not be sufficient to develop proper densification levels of the ceramic matrix. The optimal amount of liquid phase to promote densification is only reached above 1350 °C, i.e. at the temperature corresponding to the eutectic reaction in the ternary system $MgO–Al_2O_3–SiO_2$. The capillary pressure of the liquid phase acts as driving force for densification of composition C-2 and especially of composition C-3.

In C-2 and C-3 systems, cordierite phase formation seems to occur both throughout the melt and by solid-state reaction. Cordierite, mullite, anorthite and glassy phase are presented after final heat treatment at 1380 °C (composition C-2) and at 1410 °C (composition C-3).

A lower thermal expansion coefficient, better mechanical strength and volume electrical resistivity of composition C-3 (see Table 2) can be attributed to a higher content and improved crystallinity of cordierite phase.

Table 2
Properties of C-1, C-2 and C-3 samples sintered at 1350, 1380 and 1410 °C, respectively

Properties	C-1	C-2	C-3
Total shrinkage %	24.78	17.76	18.60
Water absorption %	0.12	0.30	0.10
Flexural strength MPa	62.0	64.3	91.7
Apparent density g/cm^3	2.375	2.366	2.314
Thermal expansion			
Coefficient, K^{-1} ($\times 10^6$)			
20–400 °C	1.80	1.59	1.26
20–700 °C	4.05	2.88	2.63
20–1000 °C	4.75	3.44	2.64
Volume resistivity, Ω×cm			
1000 °C	3.3×10^5	–	4.6×10^5
850 °C	$1.9\times\cdot 10^6$	–	2.5×10^6

4. Conclusion

Model systems composed of alkaline-earth-aluminosilicate glass, kaolin, alumina and magnesite were investigated to process cordierite-anorthite mixed composites at firing temperatures between 900 and 1410 °C. As predicted, the use of glass in batch formulations strongly effects the microstructure, porosity and properties of fired products. Properly sintered and dense materials consist of α-cordierite and triclinic anorthite. Decreasing of the amount of added glass promotes the formation of mullite crystals, in addition to cordierite and anorthite phases. Subsequently densification occurs due to additional liquid phase formation near the euthetic point in the ternary system $MgO–Al_2O_3–SiO_2$. Sintered materials show relatively high amounts of residual closed pores. Some experimental control of porosity evolution might be assured by changing the heating rate, as an indirect effect of the amount of formed liquid phase that is then available for bloating at high temperature. Anorthite becomes the dominant crystalline phase in these highly porous materials.

References

1. Bloor, E. C., *Ceramics a Symposium*, ed. A. T. Green and G. H. Stewart. the British Ceramic Society, Stoke-on-Trent, 1953, pp. 253–257.
2. Kleiner, R. N. and Buljan, S. T., Silicates for thermal shock resistant applications. In *Refractory Materials,* Vol. 6*, Phase Diagrams*, ed. A. M. Apler. Academic Press, New York, San Francisco, and London, 1978, pp. 313–321.
3. Udagawa, S. and Ikawa, H., Low thermal expansion ceramics. *Seramikkusu*, 1979, **14**(11), 967–976.
4. Sumi, K., Kobayashi, Y. and Kato, E., Synthesis and sintering of cordierite from ultrafine particles of magnesium hydroxide and kaolinite. *J. Am. Ceram. Soc.*, 1998, **81**(4), 1029–1032.
5. Nandi, A. K., Thermal expansion behavior of boron-doped cordierite glass-ceramics. *J. Am. Ceram. Soc.*, 1999, **82**(3), 789–790.
6. Marghussian, V. K. and Geramian, M. J., Fabrication of cordierite glass-ceramics by slip casting of glass-powders. *Br. Cera.-Trans.*, 1999, **98**(3), 133–140.
7. Ting, Ch-J., Hsi, Ch-Sh. and Lu, H.-Y., Ruthenia-based resistors and cordierite-glass substrates in low-temperature co-fired ceramics. *J. Am. Ceram. Soc.*, 2000, **83**(12), 2945–2953.
8. Insley, H. and Frechette, V. D., *Microscopy of Ceramic and Cements*. Academic Press Inc, New York, 1955.
9. Tulyaganov, D., Vargas, G., Mendez, J., Tukhtaev, M. and Johal, K., Cordierite ceramic synthesis via crystallization of alkaline-poor aluminosilicate glass. *Glastech. Ber. Glass Sci. Technol.*, 2000, **73**(C1), 36–42.
10. Tulyaganov, D., Phase equilibrium in the fluorapatite-anorthite-diopside system. *J. Am. Ceram. Soc.*, 2000, **83**(12), 3141–3146.
11. Tulyaganov, D., Glass-ceramics in the system $Ca_5[PO_4]_3F$–$CaAl_2Si_2O_8$-$CaMgSi_2O_6$. In *Ceramic Engineering and Science Proceedings,* Vol. 21*, Issue 4, 24th Annual Conference on Composites, Advanced Ceramics, Materials, and Structures*, ed. T. Jessen and E. Ustundag. American Ceramic Society, Westerville, OH, 2000, pp. 447–454.
12. Underwood, E. E., *Quantitative Stereology*. Addison-Wesley Publishing Co, Georgia, 1970.
13. Ebazadeh, T. and Lee, W. E., Processing-microstructure-property relations in mullite-cordierite composites. *J. Eur. Ceram. Soc.*, 1998, **18**, 837–848.
14. Iqbal, Y., Messer, P. F. and Lee, W. E., Non-equilibrium microstructure of bone china. *Br. Cera. Trans.*, 2000, **99**(3), 110–116.
15. Kingery, W. D., Bowen, H. K. and Vhilmann, D. R. *Introduction to Ceramics*, 2nd ed. John Wiley & Sons, Inc., 1976.
16. Osborn, E. F. and Muan, A., *Phase Equilibrium Diagrams of Oxide Systems, Plate 3*. The American Ceramic Society, Columbus, OH, 1960.